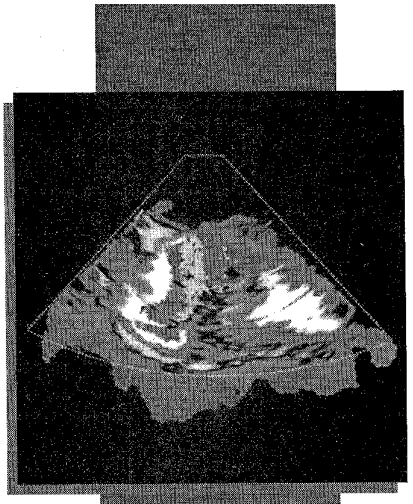

Techniques for Elastic Imaging: A Review

K.J. Parker[1,2], L. Gao[1], R.M. Lerner[3], S.F. Levinson[1,4]

[1]Dept. of Electrical Engineering and Center for Biomedical Ultrasound, University of Rochester,
[2]Dept. of Radiology, Strong Memorial Hospital
[3]Dept. of Diagnostic Radiology, Rochester General Hospital
[4]Dept. of Orthopedics, Div. of Rehabilitation Medicine, Strong Memorial Hospital

The elastic properties of tissues have become the subject of increasing research efforts. The goal of elastic imaging is to map tissue properties such as Young's modulus (or stiffness), Poisson's ratio, and viscosity in an anatomically meaningful presentation to provide useful clinical information. Perhaps the most important parameter among them is Young's modulus, because of its dependence upon the composition of the tissue. Changes in soft tissue stiffness may be related to an abnormal pathological process; for example, some tumors of the breast, liver, and prostate are detected by palpation through the overlying tissue. Physicians have relied on palpation of hard areas in tissue to aid in tumor detection; however, conventional imaging modalities display tissue parameters not directly associated with the findings on palpation.

This emerging field may be considered a merger of several related fields which have long and distinguished histories:

- The study of tissue elastic constants [biomechanics]
- The study of tissue contrast differences and tissue motion using imaging systems (x-ray, ultrasound, magnetic resonance imaging (MRI), stroboscopes and others) [radiology]
- The study of vibrating targets using coherent radiation (laser, sonar and ultrasound) [biology, physics, nondestructive testing]

In this article we review imaging techniques for assessing the elastic properties of tissue. We briefly look at the fundamental techniques in the above-mentioned fields and then present elastography techniques developed by current research groups. Our review is focused on published papers in the archival literature.

Prior Studies

The Study of Tissue Elastic Constants (Biomechanics)

A comprehensive review of this field is beyond the scope of this paper; however, some basic concepts and works directly related to elastic imaging are considered.

The stress-strain relationship for most tissues is nonlinear. Also, a hysteresis loop is encountered in cyclic loading and unloading, and stress tends to relax over time under constant strain. Many models have been proposed relating stress and strain, based on the linear theory of viscoelasticity, as classically described by Voigt, Maxwell, and Kelvin. Buchthal and Kaiser [9] proposed a model with continuous relaxation spectrum, which corresponds to a combination of an infinite number of Voigt and Maxwell elements. Viidik [64] constructed a nonlinear theory of the Kelvin type. Fung [17] formulated a quasi-linear viscoelasticity theory of soft tissue. His argument was that for oscillations of small amplitude around the equilibrium state, the theory of linear viscoelasticity should apply, while for finite deformation, his theory accounts for the nonlinear stress-strain characteristics.

Truong [63] measured the velocity and attenuation coefficient of longitudinal waves propagated along thin muscles and showed the dependence of these constants on frequency. Taber [58] studied the elastic behavior of the pig eyeball under rigid cylindrical indentures and observed the highly nonlinear stress-strain relation. Levinson [35] studied the speed of ultrasound wave propagation in frog sartorius specimens, and proposed a linear transverse anisotropic model. Parker, et al. [47], measured the linear and nonlinear Young's modulus of canine and human prostate specimens.

Although there are well-established models for measurements of elastic tissue parameters, few tissue types have been reported and there are broad gaps in our knowledge of the elastic properties of normal and diseased tissues. There is little information on the elastic properties of different components of structured organs (those containing separate regions of distinct tissue types) such as the kidney, breast, and prostate. The reaction of normal parenchyma to different tumors and lesions is also an area of unresolved speculation. Thus, there remains a need for basic measurements and characterizations of

tissue types in order to provide a foundation for modeling and interpretation of elastograms.

The Study of Tissue Motion Using an Imaging System

Oestreicher and colleagues [43, 65] studied the behavior of the human body surface subjected to sound fields or mechanical vibration. They used a strobe light and photography to acquire surface-wave propagation patterns, thus obtaining the wavelength and wave speed. They also formulated a theory to explain the increase of impedance of tissue with increased frequency. Shear modulus could be calculated from their experimental data.

Wilson and Robinson [67] presented a signal processing technique to measure small displacements of liver tissue caused by aortic pulsation and vessel diameter variations. They obtained RF (radio frequency) M-mode signals, and on the assumption that the tissue follows points of constant phase, they calculated the velocity of tissue motion from the trajectory of a constant phase point. The integral of velocity over time gave a rough estimate of displacement.

Dickinson and Hill [15] used the correlation coefficient between successive A-scans to measure the amplitude and frequency of tissue motion. They set up a correlation parameter to measure the changes of the interrogated region between two successive A-scans. The correlation parameter is unity for stationary tissue and decreases monotonically with increased tissue motion. Their assumption is that the decorrelation is proportional to displacement, which is only true for very small displacement. This technique was further developed by Tristam, et al. [61, 62], to look at the different responses of normal liver and cancerous liver to cardiac movement. They found some features on the correlation curves to distinguish between them. They found that livers with tumors generally have lower maximum values, fewer peaks, and greater regularity. De Jong, et al. [14], used a modified correlation technique to measure tissue motion, where they found the maximum cross-correlation by an interpolation algorithm. The peak location of the cross-correlation function may also be determined from several other methods, such as oversampling, sinc-interpolation, and fitting other curves like parabolas to the neighborhood of the peak of the cross-correlation function. The method of De Jong, et al. [14], is limited to narrowband signals where the cosine function still represents a good approximation.

Fetal lung elasticity may be an important indicator of pulmonary maturity and has been used to determine normal development. Birnholz and Farrell [8] tried to determine qualitatively the stiffness of a fetal lung by evaluating ultrasound B-scans, where one can see the compression of lung tissue due to cardiac pulsations. They argued that stiff lung tissue transmits cardiac pulsations, moving as a block without regional deformation, while soft lung tissue compresses with maximal deformation immediately adjacent to the heart. Adler, et al. [1,2], arrived at more quantitative estimates. They applied correlation techniques to digitized M-mode images, and estimated <r>, a parameter that characterizes the range of transmitted cardiac motion in a fetal lung. The parameter is actually the temporally and spatially averaged systolic to diastolic deformation per unit epicardial displacement.

Eisenscher, et al. [16], applied a 1.5 Hz vibration source to liver and breast tissue, and used M-mode ultrasound to look at the induced "quasistatic" compression. They found that the "quasistatic" compression response from benign lesions was characteristically sinusoidal, while that from malignant tumors tended to be more flat, i.e., more of a nonlinear response.

Krouskop, et al. [29], reported one of the first quantitative measurements of tissue elasticity using gated pulsed Doppler. The set of equations relating tissue properties and tissue movements reduces to some very simple forms under the assumption of isotropy and incompressibility, and the final problem of finding tissue elasticity reduces to measuring tissue peak displacements and their gradients. A single A-line pulsed Doppler instrument was used in their experiments to measure actual tissue motion at points of interest under external vibration. They suggested a possible measurement of tissue stiffness in a very small region, i.e., 0.5 x 0.5 mm.

The Study of Vibrating Targets Using Coherent Radiation

Laser, sonar, and ultrasound have been used to extract motion parameters of a vibrating target. The applications include military targets and nondestructive testing of devices. The typical parameters of interest are displacement amplitude, phase, and frequency. Conventional medical Doppler ultrasound is designed to characterize steady and slowly varying blood flow, and is not suitable for the detection of a vibrating target. Most of the early techniques for blood-flow measurement used frequency-domain Doppler spectral analysis to characterize the velocity profile as a function of the cardiac cycle. Detection of displacement and frequency of a vibrating target (with no steady or net displacement) requires a very different detection algorithm [37].

The Doppler spectrum of the scattered ultrasound signal from a vibrating target is similar to that of a pure-tone frequency modulation (FM) process under certain conditions. It has symmetric side harmonics around the carrier frequency. The spacing of the harmonics is equal to the target vibrating frequency, and the amplitudes of the harmonics are given by successive Bessel functions of the first kind. The expression of the signal is [59]:

$$s_r(t) = A\sum_{-\infty}^{\infty} J_n(\beta)\cos[\omega_0 t + n(\omega_L t + \varphi)] \quad (1)$$

The modulation parameter, β, of the Bessel function is proportional to the target vibrating amplitude. In this expression, ω_0 is the angular frequency of the ultrasound signal, ω_L is angular frequency of the target vibration, φ is the vibration phase, A is a constant, and the summation is taken over n harmonics of the vibration frequency.

Taylor [59, 60] used a laser Doppler technique to measure the vibrating velocity of suspended particles and to calibrate microphones. He measured the relative magnitude of the Bessel band and found the vibration amplitude by fitting the data to the theoretical spectrum.

Holen, et al. [21], observed this characteristic Bessel-band Doppler spectrum when using Doppler ultrasound to examine unusually oscillating heart valves. The Doppler spectrum changes dramatically when the product of the fast-Fourier transfrom (FFT) time and the frequency of the vibrating target varies from less than unity to larger than unity. When larger than unity, the vibration frequency of oscillating heart valves was determined by the spacing between harmonics in the Doppler spectrum. The vibration amplitude was estimated by counting the number of significant harmonics, as an approximation to the FM bandwidth, which is proportional to the amplitude of vibrations.

Cox and Rogers [13] studied the Doppler ultrasound response of fish auditory

organs to a low frequency sound field. The vibration amplitude of the hearing organ was determined by comparing the ratio of the carrier and the first side band of the Doppler spectrum. Jarzynski, et al. [25], performed a similar study using scattered laser Doppler from vibrating particles in water.

The above techniques can be classified as a "ratio method," as they are all related to some amplitude ratios of the harmonics. Huang, et al. [23], developed an estimator measuring the spectral spread (or variance) of the Doppler spectrum, which was applied for vibration amplitude imaging.

Techniques for Elastic Imaging

For centuries, physicians have used palpation to detect abnormal regions of increased Young's modulus (hardness or stiffness) as an indicator of anomolies, including cancer. The concept of elastic imaging was developed as a qualitative and quantitative technique to map tissue elasticity, thus potentially adding new clinically useful information to the interpretation of ultrasound, computed tomography (CT), or other scans. Various techniques have been developed using different modalities (ultrasound, MRI, and optics), employing different tissue excitations, and extracting different parameters of tissue motion.

Vibration Amplitude Imaging

Lerner and Parker first presented preliminary work on vibration amplitude sonoelastography ("sonoelasticity imaging") in 1987 [32]. In this method, a low-frequency vibration (20-1000 Hz) is applied externally to excite internal vibrations within the under inspection. A stiff inhomogeneity surrounded by soft tissue produces a disturbance in the normal vibration eigenmode patterns. Doppler detection algorithms are employed to make a real-time vibration image. In some organs, modal patterns can be created, revealing additional information as to the shear wave speed of sound of the tissue [46].

By 1990, the University of Rochester group was using a modified color Doppler instrument to make real-time vibration amplitude sonoelastography images, albeit "bistable" images, where vibration above a threshold produced a saturated red. Reports in 1990 described measurements of tissue elastic constants, finite element models for vibration amplitude sonoelastography, and results of phantom and ex-vivo phantom studies [34, 45]. By 1992, studies of liver, breast, and kidney tissue were published, and also a study of ex-vivo prostate cancer detection was completed [31, 46]. In 1994, a real-time, in-vitro study of the prostate had been completed, demonstrating that vibration amplitude sonoelastography had a better sensitivity and predictive value than did B-scan imaging alone [50]. Furthermore, in 1994, a mathematical model for vibration amplitude sonoelastography was completed [19]. A "sonoelastic Born" approximation was used to solve the wave equations in an inhomogeneous (but isotropic) medium. The total wave field inside the medium can be expressed as:

$$\Phi_{total} = \Phi_i + \Phi_s \tag{2}$$

where Φ_i is the homogeneous field or incident field, and Φ_s is the field scattered by the inhomogeneity. They satisfy, respectively:

$$(\nabla^2 + k)\Phi_i = 0 \tag{3}$$

$$(\nabla^2 + k)\Phi_s = \alpha(x) \tag{4}$$

where $\alpha(x)$ is a function of the properties of the inhomogeneity and k is the wave number.

Another aspect of vibration amplitude sonoelastography to be considered is the signal processing issue. Huang, et al. [23], proposed a technique to estimate β (refer to Eq. (1)) from the spectral spread. They found the simple relationship between β, which is proportional to the vibration amplitude of the target and the spectral spread, σ_ω, is.

$$\beta = \sqrt{2}(\sigma_\omega / \omega_L) \tag{5}$$

where ω_L is the vibration frequency of the vibrating target.

This is a simple but useful special property of the Bessel Doppler function. They also investigated the effect of noise, sampling, and nonlinearity on the estimation. A later paper by Huang, et al. [24], extended this work to "real-time" estimators of vibration amplitude, phase, and frequency that could be used for a variety of vibration sonoelastography techniques.

Vibration amplitude sonoelastography detects a hard lesion by looking at the disturbance of the vibration amplitude pattern. An interesting observation is that one can produce a vibration modal pattern in some organs, and these have quantitative tissue characterization applications. In practice, the lowest frequency modes are preferred, as they are the easiest to excite and to interpret. Various time and frequency estimators make this technique a real-time diagnostic tool. Vibration amplitude sonoelastography is currently in an early stage of in-vivo trials using real-time imaging techniques.

Vibration Phase Gradient Studies

Sato, et al. [54], were involved with the study of nonlinear interactions between ultrasound and lower-frequency waves in tissue at the time that Parker and Lerner, and Krouskop and Levinson, were using linear methods to investigate the propagation of vibrations inside tissue. In the late 1980s, Sato [54, 68] developed a vibration-phase gradient approach to sonoelastography, built on his and other investigators earlier works. His technique maps both the amplitude and the phase of low-frequency wave propagation inside tissue. From these maps, the wave propagation velocity and dispersion properties are derived. These parameters are directly linked to the elastic and viscous characteristics of tissue.

Because the phase-modulated (PM) Doppler spectrum of the signal returned from sinusoidally oscillating objects is similar to that of a pure-tone FM process, the tissue vibration amplitude and phase of tissue motion may be estimated from the ratios of adjacent harmonics.

From Eq. (1), the amplitude ratio between adjacent Bessel bands of the spectral of the signal is:

$$A_{i+1} / A_i = \left| J_{i+1}(\beta) / J_i(\beta) \right|. \tag{6}$$

If A_{i+1}/A_i are calculated as a function of β before hand, then β can be estimated from the experimental data.

Phase and amplitude maps constructed as a function of time permit the display of wave propagation as a moving image. Images of amplitude and phase are computed off-line using a minimum-squared-error algorithm to estimate the direction of wave propagation and to calculate phase and amplitude gradients in this direction. Preliminary in-vivo results have been demonstrated [68] under the assumption that the effect of shear viscosity is negligible at low frequencies.

Levinson [36] adapted and refined Sato's technique [68] by using a more general model of tissue viscoelasticity, and by using a linear-recursive-filtering algorithm based on cubic B-spline functions. By taking the Fourier transform of the wave equation, he found that the frequency-domain displacement equation

for a linear, homogeneous, isotropic viscoelastic material can be written as:

$$-\rho\omega^2\mathbf{U} = (\mu + i\omega\eta)\nabla^2\mathbf{U} + [(\mu+\lambda) + i\omega(\eta+\kappa)]\nabla\nabla\cdot\mathbf{U} \quad (7)$$

where **U** is the temporal Fourier transform of the internal tissue displacement, ρ is the density, μ and λ are the shear and longitudinal moduli of elasticity (also known as Lamé constants), and η and κ are the shear and longitudinal coefficients of viscosity, respectively. This equation can lead to expressions that relate the shear modulus of elasticity and viscosity to the wave number and the attenuation coefficient of the wave. It has also been suggested that these moduli could be calculated directly from Eq. (7), though methods of estimating the Laplacian in three dimensions do not currently exist.

Using the assumption that viscosity at low frequencies is negligible and that shear waves predominate, Levinson and Sato conducted a series of experiments on the quadriceps muscle group in human thighs. Values of Young's modulus of elasticity were calculated from phase-gradient images under conditions of active muscle contraction. A pulley apparatus was used to control the tension applied to the muscle. As expected, the measured speed of vibration propagation and the calculated values of Young's modulus increased with increasing degrees of contraction, as needed to counteract the applied load.

Compression Strain Studies

Ophir and colleagues [44] have developed an imaging technique ("elastography" as they named it) that is based on the static deformation of a linear, isotropic, elastic material. They externally compressed the tissue under inspection and used cross-correlation analysis on the pre- and postcompression A-line pairs. From these data, they were able to calculate the strain profile inside the tissue along the transducer axis. They measured the stress field close to the transducer surface, and added corrections for the nonuniform stress field inside the tissue. Having both strain and stress fields, they calculated the elastic modulus profile of the tissue, and displayed the information as an "elastogram."

The first RF A-line is obtained with the transducer slightly precompressing the target to ensure good contact. The second A-line is obtained after axially compressing the target an additional increment, dz (usually, dz is about 1% of the target length). The echoes are broken into small 94 mm segments overlapping 1 or 2 mm [44]). The postcompression A-line is 2dz/c shorter than the precompression A-line, where c is the speed of the ultrasound in the target. So the postcompression A-line is zero-padded to have the same length as the precompression A-line. Cross-correlation is applied between congruent segments in an A-line pair.

The temporal location of the maximum peak of the cross-correlation function is the estimate of the time shift between the two segments. The time scale is relative to the face of the transducer, so the shift of the signal starts as zero at the beginning of the A-line, and increases to $2dz/c$ at the end. If the elastic modulus differs somewhere along the line, little or no increase will show in the time shift of certain segments. After one A-line pair is processed, the corresponding strain profile was defined as a one-dimensional (1-D) graph showing the strain as a function of depth in the target. The quantity shown in Eq. (8) is a particular local estimate of the strain in the i-th depth increment:

$$s_i = \frac{t_{i+1} - t_i}{2dz/c} \quad (8)$$

Where t_i is the time shift for segment i. After repeating the process for an array of all A-lines, they obtained a strain image of the compressed target.

For stress distribution, at first they used the uniform model [44]. Later, they [49] developed a more realistic model based on Saada's [53] theory. This model accounts for the stress behavior of decaying away from the compressor, and increasing again when close to the base of the target.

As the range of strain measurement starts from zero and increases, they choose to display the inverse of elastic modulus in the "elastogram" (stiffness), so that the display has a finite range. Some phantom, in-vitro, and in-vivo experiments showed some elastic structures that do not appear on the conventional B-scan images [11]. This technique may be used to detect tumors with increased stiffness inside compressible soft tissue.

There are some signal processing issues and artifacts associated with the cross-correlation method mentioned above. The estimation of the time shift tends to favor regions with large envelope amplitude within the estimation window. Céspedes and Ophir [11] proposed a pre-cross-correlation amplitude compression technique to reduce these artifacts, and they also proposed a signal stretching method.

Since cross-correlation is used to analyze A-line pairs to obtain strain information in this technique, an approximate stress distribution inside tissue has to be assumed for final elasticity reconstruction. The basic model is two-dimensional. Data processing is done off-line. Preliminary in-vivo results are also shown in [11].

Multiple-step Compression-strain Sonoelastography

A group at the University of Michigan, Ann Arbor, headed by O'Donnell, has developed an approach to compression strain sonoelastography. They presented a 2-D analytical model for the "forward problem" [42, 57]. That is, given Young's modulus as a function of position, to predict the strain inside tissue given specific forces and boundary conditions. The governing equations for static deformation of an isotropic, viscoelastic, and incompressible medium were derived from Newton's second law, incompressibility, and stress-strain relationships. The simplified 2-D equations are:

$$\frac{\partial p}{\partial x_1} + 2\frac{\partial}{\partial x_1}\left(\mu\frac{\partial u_1}{\partial x_1}\right) + \frac{\partial}{\partial x_2}\left(\mu\left(\frac{\partial u_1}{\partial x_2} + \frac{\partial u_2}{\partial x_1}\right)\right) = 0 \quad (9a)$$

$$\frac{\partial p}{\partial x_2} + 2\frac{\partial}{\partial x_2}\left(\mu\frac{\partial u_2}{\partial x_2}\right) + \frac{\partial}{\partial x_1}\left(\mu\left(\frac{\partial u_1}{\partial x_2} + \frac{\partial u_2}{\partial x_1}\right)\right) + f_2 = 0 \quad (9b)$$

$$\frac{\partial u_1}{\partial x_1} + \frac{\partial u_2}{\partial x_2} = 0 \quad (9c)$$

where u_1 and u_2 are displacements for each point along x_1 and x_2 directions, respectively. μ is proportional to Young's modulus, p is static internal pressure, and f_2 is the body force. This set of equations with boundary conditions cannot be solved analytically except for very few extreme situations, so a finite difference method was used to obtain the solution iteratively.

The technique, used to detect the strain inside the medium after deformation, is based on cross-correlation of ultrasound A-lines. The group suggested using large deformation to maximize the signal-to-noise ratio (SNR) of the displacement and

strain estimations. However, large displacement (over 10 wavelengths of the carrier signal) results in significant internal strain, which changes the spatial distribution of the scatterers within an area of the image, thus decorrelating the speckle patterns used for cross-correlation. Instead, they used multiple small step deformations (each step was less than one wavelength) to produce a large total deformation. The total displacement was then calculated by accumulating the displacement between each small deformation.

For signal processing, they used baseband (not RF) correlation to determine the displacement inside the tissue after each small deformation. The time shift between the pre- and postdeformation signals was estimated from the phase of their zero-lag correlation functions:

$$t_{BB} = \frac{\tan^{-1}\left[\dfrac{\mathrm{Im}(\tilde{C}(0))}{\mathrm{Re}(\tilde{C}(0))}\right]}{\omega_0} \qquad (10)$$

where $\tilde{C}$ is the baseband correlation function. A limitation associated with phase processing is that aliasing occurs if the displacement exceeds a quarter of an ultrasound wavelength. To overcome this limitation, they evaluated the differential displacement between neighboring vertical pixels, and then integrated it starting at a known position. Low-pass filtering prior to phase detection can help to obtain better results. The vertical strain is the spatial derivative of vertical displacement. In this case, differential displacement was already calculated, so the strain was easily obtained.

Some preliminary results on reconstructing elasticity images were given in their other publications [41]. Kelle, et al. [28], have suggested other reconstruction schemes. This group of investigators also posed the inverse problem: to construct a Young's modulus image given strain images. As the technique uses finite difference calculations, the solution may not converge if the initial guess is inadequate. In this approach, baseband correlation between A-line pairs is employed to estimate displacement. Multiple steps of compression are used to reduce the speckle decorrelation effect. The basic model is 2-D and the data processing is done off-line. Phantom and some in-vitro results are presented.

Inherent Strain Studies

Bertrand and colleagues proposed a biomechanical strain gauge using B-scan information and an optical-flow algorithm [7]. They modeled tissue deformation on consecutive B-scan images as linear transformations [7, 27, 39]. These transformations can be decomposed into rotation matrices and biaxial translation matrices. By calculating the eigenvalues of these matrices in a small region, the strain in that region can be obtained. They suggested further application of this technique to elasticity estimates of skeletal muscles, and also described an important artifact in apparent speckle motion during tissue rotation [28].

Tissue Motion with Speckle Tracking

Trahey and his colleagues [66] have developed a 2-D speckle tracking technique to measure blood flow and motion in soft tissue. The speckle tracking system employed a sum of absolute difference (SAD) method to estimate tissue motion in two dimensions. The echo data was first obtained for a 2-D "kernel" region of size $m \times n$: $k(i,j)$. At a later time, the data for a "search" region including and surrounding the kernel region was acquired: $s(i,j)$. The following equation was evaluated for each a and b until a minimum of $\varepsilon(a,b)$ occurred:

$$\varepsilon(a,b) = \sum_{i=1}^{m}\sum_{j=1}^{n}\left|k(i,j) - s(i+\mathrm{a}, j+b)\right| \qquad (11)$$

Then, (a,b) was the movement of the "kernel" region between the time of the first and the second data acquisitions.

In an application to vibration amplitude sonoelastography [66], they measured tissue motion excited by externally applied vibration. Their system utilized three major components: an electromechanical vibrator to excite tissue motion, an ultrasound scanner that can output either RF or detected echo data, and a speckle tracking system for motion estimation. Synchronization was made between the three components so that phase information was preserved. The 2-D displacement information was displayed in real-time as 2-D map of colors.

Other Quantitative Characterization Techniques

In this section, we summarize other recent developments related to measurements of local elastic properties and tissue motion.

Characterization of Elastic Vessels

Javier and Pedersen [26] studied an elasticity parameter of an elastic tube (the apparent compliance). They used ultrasound pulse-echo to measure the diameter variation of the tube in response to externally applied time-varying pressure functions.

In the experiments, they first used pulse-echo to obtain reference signals from the back and front walls of a latex tube under ambient pressure. A sinusoidally varying pressure was then applied to the tube, and the echoed signals were cross-correlated to the reference signals. Given the knowledge of the ultrasound propagation speed, the diameter change of the tube was easily estimated using these cross-correlations.

They made measurements along a 20 cm-long tube under different forcing frequencies. Some interesting observations are: 1) the tube has apparent resonant frequencies and 2) the diameter variation decreases at the location of increased stiffness. The localized increase in tube stiffness may serve as a simple model for vessel pathology such as arteriosclerosis.

A group in Toronto headed by Foster [51, 52] also studied vessel-wall displacement under applied pressure. They placed a radially oriented 42 MHz single-element transducer inside the tube under study. Complete cross-sectional scans were acquired by rotating the transducer outer housing through 360°. A correlation search technique was also employed to assess the tube-wall displacement. They claimed a system-detection sensitivity of 10 μm axially and 20 μm laterally. The data processing, including correlation searching, was done off-line.

Fetal Movements

There have been further developments in the study of fetal lung movement. Fetal movement reflects fetal and neural conditions, and evaluation of this movement may be valuable in the management of high-risk pregnancy. Shinozuka and Yamakoshi [55, 56] used a multichannel pulsed Doppler system to monitor fetal movements. Each channel processed signals echoed from one point inside the fetus along the ultrasound beam direction, with points separated by 1.5 cm. The displacements were estimated by an arc-tangent method, that is, calculating the phase shift from the quadrature components of the signal by:

$$\Delta x = \frac{c}{2\omega}\left\{\tan^{-1}\left(\frac{Q(t)}{I(t)}\right) \pm n\pi\right\} \qquad (12)$$

where c is the speed of ultrasound, ω is the frequency, and $Q(t)$ and $I(t)$ are the quadrature and in-phase components of the signal, respectively. $n\pi$ is used to offset the displacement from zero-crossing points of $I(t)$. They also classified the characteristics of three different movements: fetal breath movement (FBM), fetal gross movement (FGM), and fetal heart movement (FHM), based on the different frequency ranges and amplitudes of the movements. Then they used the maximum entropy method to separate these different movements.

Tissue Motion With MRI

Zerhouni, et al. [70], proposed a tagging MRI technique to assess myocardial motion. A key procedure in this technique is to apply a selective RF pulse to sections of tissue before imaging, which is done in the presence of a linear magnetic-gradient field, so the magnetization of protons in those sections are perturbed. Before the full recovery of magnetization, an MR image of the tissue is obtained in a plane orthogonal to the tagged planes. Due to the different degrees of saturation, the signals will be different between the tagged and un-tagged regions. The motion occurring during the tagging and imaging interval will be reflected by the displacement and distortion of the tagged regions. Some studies using a similar technique have also been reported by Axel and Dougherty [5, 6]. A very recent work from the Mayo Clinic reports a direct MRI visualization of shear waves [40].

Measurement of Intraocular Pressure

Richards and collaborators [3, 4] have applied vibration amplitude sonoelastography to the eye with a goal of detecting intraocular pressure (IOP). The basic postulate is that the sclera is a tough, nonlinear elastic shell with spherical geometry. Natural resonances of the eye can be excited at different frequencies and detected by Doppler ultrasound. As IOP increases, the sclera stiffens appreciably, shifting the resonance frequencies of the eye. Preliminary in-vitro and in-vivo results have supported the basic concept; however, the accuracy of the technique in clinical use remains to be studied.

Conclusion

Tissue elasticity has always been an important concept in the fields of medicine and biology. The combination of this concept with modern imaging systems creates elasticity imaging techniques. Although these techniques still require further development, work to date has established potential for useful clinical diagnostic information that cannot be obtained by traditional imaging.

A number of issues remain unanswered and require further study before imaging techniques are optimized and can be introduced into clinical use. Some of these issues are:

- Elasticity data. There is a great need for reliable measurements of the elastic properties of tissue in normal and different pathological conditions. These data are critical to the generation, evaluation and interpretation of different strategies.
- Source excitation. In both static measurements and dynamic (vibration) sonoelastography, there is a need to optimize the source of mechanical excitation in spatial and temporal (frequency) terms. The goal is to optimize the resulting image and permit the best possible interpretation of the underlying pathology.
- Tissue models. Early models assumed simple linear isotropic elastic behavior. The appropriateness and limitation of these simple models require further examination, in view of the widespread recognition of the complicated nature of tissues, including nonlinear behavior, hysteresis effects, and complex viscoelastic temporal response.
- Boundary conditions. The nature of organ-organ or tissue-tissue boundary conditions is not well understood. These are important in a wide range of compression and vibration sonoelastography applications. Do fat globules slip out-of-plane in different loading conditions? How well can displacements (or shear waves) be transmitted across the liver-kidney boundary? These questions will require careful experimental and theoretical treatment.

The early applications of sonoelastography have been quite promising, and the results clearly indicate that new information, previously unavailable in conventional imaging modalities, can now be obtained.

Acknowledgments

Support from NSF/NYS Center for Electronic Imaging Systems is gratefully acknowledged. We appreciate the advice from Dr. S.K. Alam and Dr. D. Rubens in preparing the article.

Kevin J. Parker received the B.S. degree in engineering science, summa cum laude, from SUNY at Buffalo in 1976. Graduate work in electrical engineering was done at MIT, with M.S. and Ph.D. degrees received in 1978 and 1981. He is currently professor of electrical enigneering and radiology and director of the Rochester Center for Biomedical Ultrasound. Dr. Parker has received awards from the National Institute of General Medical Sciences (1979), the Lilly Teaching Endowment (1982), the IBM Supercomputing Competition (1989), and the World Federation of Ultrasound in Medicine and Biology (1991). He has been named a fellow in both the IEEE and the AIUM for his work in medical imaging. In addition, he was recently named to the Board of Governors of the AIUM. Dr. Parker's research interests are in medical imaging, linear and nonlinear acoustics, and digital halftoning.

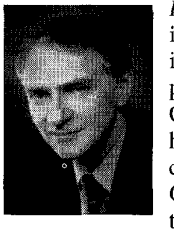

Robert M. Lerner, born in Newark, New Jersey, in 1945, received his primary education in Columbus, Ohio. He holds degrees in Electrical Engineering from General Motors Institute (B.E.E., 1969), the University of Michigan (M.S.E., 1968) and University of Rochester (Ph.D., 1978). He also received the M.D. degree in 1977 while in the combined M.D.-Ph.D. Program at the University of Rochester. From 1968 to 1972 he was a Research Engineer in the Physics Department at General Motors Research Laboratories. Following medical school, Dr. Lerner completed his residency in Diagnostic Radiology at the University of Rochester in 1981. Subsequently, he joined the faculty in the Diagnostic Radiology Department at the University of Rochester and directed the Ultrasound Section of Strong Memorial Hospital until 1990. He now directs the Ultrasound Section of the Diagnostic Radiology Department at Rochester General Hospital in Rochester, New York. He is an Adjunct Associate Professor of Diagnostic Radiology and continues to be actively involved in ultrasound research and is a member of the Rochester Center for Biomedical Ul-

trasound. Dr. Lerner is a fellow of the American Institute of Ultrasound in Medicine and a member of the Radiological Society of North America and the American Roentgen Ray Society.

Stephen F. Levinson, M.D., Ph.D., received the B.S. and M.S.E. degrees in Interdisciplinary Engineering from Purdue University in 1976 and 1978, respectively. He went on to complete a Ph.D. in Electrical Engineering from Purdue in 1981 and an M.D. from Indiana University in 1983 as part of a combined degree program. Though never intending to practice medicine, his research and clinical interests led to the completion of a residency in Physical Medicine and Rehabilitation at Stanford University in 1986, and a staff position at the NIH Clinical Center. Since 1992, he has been a member of the clinical faculty in the Department of Physical Medicine and Rehabilitation at the University of Rochester, with a joint appointment in the Department of Electrical Engineering. His research interests for the past 20 years have focused on the propagation of ultrasound in skeletal muscle. One of the first to develop techniques of sonoelastography, he is currently seeking to develop dynamic imaging methods suitable for the study of human muscle.

Address for Correspondence: Kevin J. Parker, Professor and Chair, Dept. of Electrical Engineering, University of Rochester, Rochester, NY 14627.

References

1. **Adler R, Rubin JM, Bland P, Carson P:** Characterization of transmitted motion in fetal lung: quantitative analysis. *Med Phys* 16:333-337, 1989.

2. **Adler RS, Barbosa DC, Cosgrove DO, Nassiri DK, Bamber JC, Hill CR:** Quantitative tissue motion analysis of digitized M-mode images: gestational differences of fetal lung. *Ultrasound Med Biol* 16:561-569, 1990.

3. **Alam SK, Richards DW, Parker KJ:** Detection of intraocular pressure change in a human eye model using sonoelastic Doppler ultrasound. Proceedings *IEEE Ultrasonic Symposium*, 1992 pp. 1057-1060.

4. **Alam SK, Richards DW, Parker KJ:** Detection of intraocular pressure change in the eye using sonoelastic Doppler ultrasound. *Ultrasound Med Bio* 20: 751-758, 1994.

5. **Axel L, Dougherty L:** Heart wall motion: improved method of spatial modulation of magnetization for MR imaging. *Radiology* 172: 349-350, 1989.

6. **Axel L, Dougherty L:** MR imaging of motion with spatial modulation of magnetization. *Radiology* 171: 841-845, 1989.

7. **Bertrand M, Meunier J, Doucet, Ferland G:** Ultrasonic biomechanical strain gauge based on speckle tracking. Proceedings IEEE Ultrasonics Symposium, pp. 859-863, 1989.

8. **Birnholz JC, Farrell EE:** Fetal lung development: compressibility as a measure of maturity. *Radiology* 157:495-498, 1985.

9. **Buchtal F, Kaiser E:** The rheology of the cross striated muscle fibre with particular reference to isotonic conditions. Det Kongelige Danske Videnskabernes Selskab, Copenhagen, *Dan Biol Med* 21:328, 1951.

10. **Carstensen E, Schwan H:** Acoustic properties of hemoglobin solutions. *J Acoust Soc Am* 31:305-311, 1959.

11. **Céspedes I, Ophir J:** Reduction of image noise in elastography. *Ultrasonic Imaging* 15:89-102, 1993.

12. **Céspedes I, Ophir J, Ponnekanti H** and **Maklad N:** Elastography: Elasticity imaging using ultrasound with application to muscle and breast in vivo. *Ultrasonic Imaging* 15:73-88, 1993.

13. **Cox M, Rogers PH:** Automated noninvasivemotion measurement of auditory organs in fish using ultrasound. *Journal of Vibration, Acoustics, Stress, and Reliability in Design* 109:55-59, 1987.

14. **DeJong PGM, Arts T, Hoeks APG, Reneman RS:** Determination of tissue motion velocity by correlation interpolation of pulsed ultrasonic echo signals. *Ultrasonic Imaging* 12:84-98, 1990.

15. **Dickinson RJ, Hill CR:** Measurement of soft tissue motion using correlation between A-scans. *Ultrasound Med and Biol* 8:263-271, 1982.

16. **Eisensher A, Schweg-Toffler E, Pelletier G, Jacquemard G:** La palpation échographique rythmée-echosismographie. *Journal de Radiologie* 64:255-261, 1983.

17. **Fung YC:** Biomechanics - Mechanical Properties of living tissues. Springer-Verlag Inc., New York, NY, 1981.

18. **Gao L, Alam SK, Parker KJ:** A new vibration theory for Sonoelasticity imaging. *Proceedings IEEE Ultrasonics Symposium* 2: 879-882, 1993.

19. **Gao L, Alam SK, Lerner RM, Parker KJ:** Sonoelasticity imaging: theory and experimental verification. *J Acoust Soc Am*, in press.

20. **Gradshteyn IS, Ryzhik IM:** Table of integrals series and products. Academic Press Inc. U.S.A. (Translated from the Russian by Scripta Technica Inc.) pp. 480, 1965.

21. **Holen J, Waag RC, Gramiak R:** Representation of rapidly oscillating structures on the Doppler display. *Ultrasound Med Biol* 11:267-272, 1985.

22. **Huang SR:** Principles of sonoelasticity imaging and its applications in hard tumor detection. Ph.D. thesis, University of Rochester, Rochester, New York, 1990.

23. **Huang SR, Lerner RM, Parker KJ:** On estimating the amplitude of harmonic vibration from the Doppler spectrum of reflected signals. *J Acoust Soc Am* 88:310-317, 1990.

24. **Huang SR, Lerner RM, Parker KJ:** Time domain Doppler estimators of the amplitude of vibrating targets. *J Acoust Soc Am* 91:965-974, 1992.

25. **Jarzynski J, Lee D, Vignola J, Berthelot H, Pierce AD:** Fiber optics Doppler systems for remote sensing of fluid flow. Ocean Optics IX, *Proceedings of SPIE Conference on Optics, Electro-Optics, and Sensors*, Vol. 925, pp. 250-254, SPIE, Apr. 4-6, 1988.

26. **Javier CB, Pedersen CP:** Ultrasonic measurement of forced diameter variations in an elastic tube. *Ultrasonic Imaging* 16, 124-142, 1994.

27. **Kallel F, Bertrand MA:** Note on strain estimation using correlation techniques. *IEEE Proceedings Ultrasonics Symposium*, 883-887, 1993

28. **Kallel F, Bertrand M, Meunier J:** Speckle motion artifact under tissue rotation. *IEEE Trans Ultrasonic Ferroelec Freq Cont* 41:105-122, 1994.

29. **Krouskop TA, Dougherty DR,** Levinson SF: A pulsed Doppler ultrasonic system for making noninvasive measurements of the mechanical properties of soft tissues. *J Rehabilitation Res Biol* 14:1-8, 1987.

30. **Laurence NB, Trahey GE:** A novel method for angle independent ultrasonic imaging of blood flow and tissue motion. IEEE Trans Biomed Eng 38:280-286, 1991.

31. **Lee F, Bronson JP, Lerner RM, Parker KJ, Huang SR, Roach, DJ:** Sonoelasticity imaging: results in vitro tissue specimens. *Radiology* 181:237-239, 1991.

32. **Lerner RM, Parker KJ:** Sonoelasiticity images, ultrasonic tissue characterization and echo graphic imaging. In *Proceedings of the 7th European Communities Workshop*. Nijmegen, The Netherlands, 1987.

33. **Lerner RM, Parker KJ, Holen J, Gramiak R, Waag RC:** Sono-elasticity: Medical elasticity images derived from ultrasound signals in mechanically vibrated targets. *Acoustical Imaging*, Vol. 16, 1988.

34. **Lerner RM, Huang SR, Parker KJ:** Sonoelasticity images derived from ultrasound signals in mechanically vibrated tissues. *Ultrasound Med Biol* 16:231-239, 1990.

35. **Levinson SF:** Ultrasound Propagation in Anisotropic Soft Tissues: the Application of Linear Elastic Theory. *J Biomechanics* 20:251-260, 1987.

36. **Levinson SF, Shinagawa M, Sato T:** Sonoelastic determination of human skeletal muscle elasticity. *J Biomechanics* (accepted for publication).

37. **McVeigh ER, Zerhouni EA:** Noninvasive measurement of transmural gradients in myocardial strain with MR imaging. *Radiology*, 180: 677-683, 1991.

38. **Meunier J, Bertrand M:** Ultrasonics speckle motion inherent to tissue motion: theory and simulation. *Proceedings IEEE Ultrasonics Symposium*, 865-868, 1989.

39. **Meunier J, Bertrand M, Faouzi K:** A model of speckle motion artifacts occurring under tissue linear transformation. *Ultrasonic Imaging* 11:133, 1989.

40. **Muthupilli R, Lomas D, Rossman P, Greenleaf J, Manduca A, Ehman R:** MR Elastography by direct visualization of propagating acoustic strain waves. *Science* 269:1854-1856, 1995.

41. **O'Donnell M, Emelianov SY, Skovoroda AR, Lubinski MA, Weitzel WF, Wiggins RC:**

Quantitative elasticity imaging. *Proceedings IEEE Ultrasonics Symposium* 2: 893-903, 1993.

42. **O'Donnell M, Skovoroda AR, Shapo BM,** and **Emelianov SY:** Internal displacement and strain imaging using ultrasonic speckle tracking. *IEEE Trans Ultrasonics Ferroelect Freq Contr* 41: 314-325, 1994.

43. **Oestreicher HL:** Field and impedance of an oscillating sphere in a viscoelastic medium with an application to biophysics. *J Acoust Soc Am* 23:707-714, 1951.

44. **Ophir J, Céspedes I, Ponnekanti H, Yazdi Y, Li X:** Elastography: a quantitative method for imaging the elasticity of biological tissues. *Ultrasonic Imaging* 13:111-134, 1991.

45. **Parker KJ, Huang SR, Musulin RA:** Tissue response to mechanical vibrations for sonoelasticity imaging. *Ultrasound Med Biol* 16:241-246, 1990.

46. **Parker KJ, Lerner RM:** Sonoelasticity of organs: shear waves ring a bell. *J Ultrasound Med* 11:387-392, 1992.

47. **Parker KJ, Huang SR, Lerner RM, Lee F Jr, Rubens D, Roach D:** Elastic and ultrasonic properties of the prostate. Proceedings IEEE Ultrasonics Symposium 2:1035-1037, 1993.

48. **Pauly H, Schwan H:** Mechanism of absorption of ultrasound in liver tissues. *J Acoust Soc Am* 50:692-699, 1971.

49. **Ponnekanti H, Ophir J, Céspedes I:** Axial stress distributions between coaxial compressors in elastography: an analytical model. *Ultrasound Med Biol* 18, 667-673, 1992.

50. **Rubens DJ, Hadley MA, Alam SK, Gao L, Mayer RD, Parker KJ:** Sonoelastic imaging of prostate cancer: in vitro results. *Radiology*, in press.

51. **Ryan LK, Lockwood GR, Starkoski BG, Holdsworth DW, Rickey DW, Drangova M, Fenster A** and **Foster FS:** A high frequency intravascular imaging system for investigation of vessel wall properties. *Proceedings IEEE Ultrasonics Symposium 2*: 1101-1105, 1992.

52. **Ryan LK, Lockwood GR, Bloomfiled TS, Foster FS:** Speckle tracking in high frequency ultrasound images with application to intravascular imaging. *Proceedings IEEE Ultrasonics Symposium 2:* 889-892, 1993.

53. **Saada AS:** *Elasticity, Theory and Applications*. Pergamon Press, New York; pp. 395-428, 1974.

54. **Sato T, Fukusima A, Ichida N, Ishikawa H, Miwa H, Igarashi Y, Shimura T, Murakami K:** Nonlinear parameter tomography system using counterpropagating probe and pump waves. *Ultrasonic Imaging* 7:49-59, 1985.

55. **Shinozuka N, Yamakoshi Y.** Measurement of fetal movements using multichannel ultrasound pulsed Doppler: autorecognition of fetal movements by maximum entropy method. *Med and Biol Eng and Comput*_31:S59-S66, 1993.

56. **Shinozuka N, Yamakoshi Y, Taketani Y:** New method for tracking fetal breathing movements using real-time pulsed Doppler ultrasonographic displacement measurement. *J Ultrasound Med* 13:19-25, 1994.

57. **Skovoroda AR, Emelianov SY, Lubinski MA, Sarvazyan AP, O'Donnell M:** Theoretical analysis and verification of ultrasound displacement and strain imaging. *IEEE Trans Ultrasonics Ferroelec Freq Contr* 41:302-313, 1994.

58. **Taber LA:** Large deformation mechanics of the enucleated eyeball. *J Biomechanical Eng* 106:229-234, 1984.

59. **Taylor KJ:** Absolute measurement of acoustic particle velocity. *J Acoust Soc Am* 59:691-694, 1976.

60. **Taylor KJ:** Absolute calibration of microphones by a laser-Doppler technique. *J Acoust Soc Am* 70:939-945, 1981.

61. **Tristam M, Barbosa DC, Cosgrove DO, Nassiri DK, Bamber JC, Hill CR:** Ultrasonic study of in vivo kinetic characteristics of human tissues. *Ultrasound Med Biol* 12:927-937, 1986.

62. **Tristam M, Barbosa DC, Cosgrove DO, Nassiri DK, Bamber JC, Hill CR:** Application of Fourier analysis to clinical study of patterns of tissue movement. *Ultrasound Med Biol* 14:695-707, 1988.

63. **Truong XT:** Extensional wave-propagation characteristics in striated muscle. *J Acoust Soc Am*, 51, 1352-1356, 1971.

64. **Viidik A:** Biomechanics and functional adaptation of tendons and joint ligaments. Studies on the anatomy and function of bone and joints. Evans, F. G. (ed) Springer-Verlag, New York, pp. 17-39, 1966.

65. **Von Gierke HE, Oestreicher HL, Franke EK, Parrack HO, Von Wittern WW:** Physics of vibrations in living tissues. *J Appl Physiol* 4:886-900, 1952.

66. **Walker WF, Friemel BH, Laurence NB, Trahey GE:** Real-time imaging of tissue vibration using a two-dimensional speckle tracking system. Proceedings 1993 IEEE Ultrasonics Symposium. 873-877, 1993.

67. **Wilson LS, Robinson DE:** Ultrasonic measurement of small displacements and deformations of tissue. *Ultrasonic Imaging* 4:71-82, 1982.

68. **Yamakoshi Y, Sato J, Sato T:** Ultrasonic imaging of internal vibration of soft tissue under forced vibration. *IEEE Trans. Ultrasonics Ferroelectr. Freq. Contr.* 37:45-53, 1990.

69. **Yemelyanov SY, Skovoroda AR, Lubinski MA, Shapo BM, O'Donnell M:** Ultrasound elasticity imaging using Fourier based speckle tracking algorithm. Proceedings 1992 IEEE Ultrasonics Symposium 2:1065-1068, 1992.

70. **Zerhouni EA, Parish DM, Rogers WJ, Yang A, Shapiro EP:** Human heart: tagging with MR imaging - A method for noninvasive assessment of myocardial motion. *Radiology* 169: 59-63, 1988.